

Aircraft-based observations and high-resolution simulations of an Icelandic dust storm

A.-M. Blechschmidt^{1,*}, J. E. Kristjánsson¹, H. Ólafsson^{2,3}, J. F. Burkhardt⁴, and Ø. Hodnebrog¹

¹Department of Geosciences, University of Oslo, Oslo, Norway

²Department of Physics, University of Iceland, Reykjavik, Iceland

³Geophysical Institute, University of Bergen, Bergen, Norway

⁴Norwegian Institute for Air Research (NILU), Kjeller, Norway

* now at: NCAS-Weather, University of Lancaster, Lancaster, United Kingdom

Abstract. The first aircraft-based observations of an Icelandic dust storm are presented. The measurements were carried out over the ocean near Iceland's south coast in February 2007. This dust event occurred in conjunction with an easterly barrier jet of more than 30 m/s. The aircraft measurements show high particle mass mixing ratios in an area of low wind speeds in the wake of Iceland near the coast, decreasing abruptly towards the jet. Simulations from the Weather Research and Forecasting Model coupled with Chemistry (WRF/Chem) indicate that the measured high mass mixing ratios and observed low visibility inside the wake are due to dust transported from Icelandic sand fields towards the ocean. This is confirmed by meteorological station data. Primary dust sources are glacial outwash terrains located near the Mýrdalsjökull glacier. Sea salt aerosols produced by the impact of strong winds on the ocean surface started to dominate as the aircraft flew away from Iceland into the jet. The present results support recent studies which suggest that Icelandic deserts should be considered as important dust sources in global and regional climate models.

1 Introduction

Iceland has over 20 000 km² of sandy deserts (Arnalds et al., 2001). The sand originates to a large extent from volcanic fly ash and glacial outwash. In particular, volcanic eruptions can cause glacial melting and flooding which leaves behind large amounts of sandy material. Water erosion is the dominant erosion type in southwest Iceland (Arnalds, 2000).

Due to its location inside the North Atlantic storm track, Iceland is frequently affected by synoptic scale cyclones. Together with the effect of Iceland's orography on the airflow, this favors the development of high wind speeds in the vicinity

of the sandy areas. The latter can, under dry, snow-free conditions lead to sand storms. Wind erosion in Iceland is very effective in transporting soil material (Ingólfsson, 2008). Maps showing sandy areas, major plume areas and deposition areas in Iceland are given by Arnalds (2010).

Iceland experiences considerable amounts of precipitation throughout the year (Crochet et al., 2007; Rognvaldsson et al., 2007). However, it is a substantial global dust source with deposition rates comparable to or higher than those found for other areas that are usually considered to contribute to major global dust emissions (Arnalds, 2010; Prospero et al., 2012).

Icelandic dust plumes can be transported over large distances and may affect air quality of the British Isles, continental Europe and the higher latitudes (Ovadnevaite et al., 2009; Prospero et al., 2008; Prospero et al., 2012). Recently, Thorsteinsson et al. (2011) found that dust storms were important contributors to an exceedance of health limit PM₁₀ concentrations measured near Reykjavík during 2007 and 2008. Prospero et al. (2012) investigated measurements from an aerosol sampling site on Heimaey island located near Iceland's south coast between 1997 and 2004. The records revealed that dust was present year-round at concentrations of a few micrograms per cubic meter, but with occasional peaks of up to 1400 $\mu\text{g}/\text{m}^3$. Using a combination of satellite images and a Lagrangian trajectory model, Prospero et al. (2012) attributed all of their dust measurements to dust storms in southern Iceland.

In addition to studies on Icelandic dust storms, ash transport from Icelandic volcanic eruptions has also been investigated (e.g. Schumann et al., 2011).

We hereby present, to our knowledge, the first aircraft-based study of an Icelandic dust storm. The measurements were carried out during flight B269 of the GFDex (Greenland Flow Distortion experiment; Renfrew et al., 2008) on 22 February 2007, with the Facility for Airborne Atmospheric Measurements (FAAM) BAE 146 aircraft. The dust storm occurred during a South Iceland low-level barrier jet event

(see Figure 1 for a map of the wind field). The jet with near-surface winds of about 30 m/s was caused by orographic distortion of a northeasterly flow of 10–15 m/s, which was caused by a combination of a low pressure area to the south of Iceland and high pressure over Greenland. The flow distortion is particularly pronounced due to a combination of large static stability (N), weak to moderate winds (U) and high mountains over southeastern Iceland (h), as indicated by high values of the inverse Froude number Nh/U (Ólafsson et al., manuscript in preparation). Wind speed maxima occurred downstream of the glaciers Mýrdalsjökull and Vatnajökull (see Figure 2 for the location of these glaciers). A detailed description of the formation, meteorological conditions and characteristics of the wake and jet is given by Ólafsson et al. (manuscript in preparation).

Figure 2 shows the aircraft track. While the flight started at unlimited visibility at Keflavík, researchers aboard the aircraft were caught by surprise as they flew into very low visibility inside the wake (see Figure 3 (a)). The visibility decreased sharply towards the coast. The sea-surface inside the wake was almost completely calm and wind speeds reached only a few m/s. The view changed completely inside the jet (see Figure 3 (b)) where strong winds around 30 m/s roughened the sea surface producing intense sea-spray. The wake and barrier jet region were investigated at three different heights: 1900 m (leg 3), 700 m (leg 4) and 400 m (leg 5). In the present paper, only measurements from these flight legs, covering the jet and the wake, are discussed. However, as can be seen on further pictures taken aboard the aircraft (not shown), the low visibility was most pronounced at the lower elevation legs (leg 4 and leg 5).

Two manned meteorological stations located to the south of the glacier Mýrdalsjökull and at Heimaey (see black stars in Figure 8 for the location of these stations) reported widespread dust on the flight day, accompanied by visibilities well below 10 km in the absence of fog or precipitation.

The primary objective of flight B269 was to investigate meteorological conditions inside the jet and in the accompanying region of low wind speeds inside Iceland's wake. The dust storm itself was not foreseen by the researchers on the aircraft. Hence, the aircraft was not equipped for measurements of a sand storm. That is why only limited information on aerosols is available. Nonetheless, important measurements of particle mass mixing ratio and particle concentration were carried out. The Weather Research and Forecasting model coupled with Chemistry (WRF/Chem) is used in the present study to better characterise the type of particles sampled by the aircraft. Aircraft measurements indicate that anthropogenic and fire emissions did not contribute to the low visibility observed near Iceland. The WRF/Chem simulations focus on dust and sea salt aerosols which is in agreement with the observations described above. The Lagrangian transport model FLEXPART is used here to identify primary source regions of air masses measured aboard the FAAM flight.

Aircraft data and model configurations will be described in section 2 and 3, respectively. Simulations and measurements are then compared and discussed in section 4, followed by a brief section on satellite lidar observations (5). Finally, summary and conclusions are given in section 6.

2 Aircraft data

A suite of instruments were carried on the FAAM aircraft. Only some of them which are related to particles are described here. For a complete list of core instrumentation see Renfrew et al. (2008) and <http://www.faam.ac.uk/>. The aircraft data were provided by the British Atmospheric Data Centre (BADC) through their web site at <http://badc.nerc.ac.uk/home/index.html>.

The Passive Cavity Aerosol Spectrometer Probe (PCASP) is an optical particle counter which counts and sizes aerosols in 15 channels between 0.1 μm and 3.0 μm diameter. The instrument measures the intensity of light backscattered by particles that pass a laser beam. Particles are dried as they are focused into the laser beam. However, large measurement errors can occur in cases of particularly moist aerosols, if measurements are carried out inside a cloud or if water droplets shatter on the inlet probe (Taylor et al., 2000).

The two-dimensional cloud particle imaging probe (2DC) and precipitation particle imaging probe (2DP) measure cloud and precipitation drop size distributions, respectively. Both instruments produce two-dimensional shadow images of particles which pass a laser beam (<http://www.eol.ucar.edu/raf/Bulletins/B24/2dProbes.html>). The 2DC probe covers diameters from 25 μm to 800 μm , while 2DP covers larger diameters between 200 μm and 6400 μm .

3 Model configurations

3.1 WRF/Chem

The Weather Research and Forecasting (WRF) model is a mesoscale numerical weather prediction and atmospheric simulation system which was developed at the National Center for Atmospheric Research (NCAR) (Skamarock et al., 2008). In WRF/Chem (Grell et al., 2005) an atmospheric chemistry module is fully coupled online with the WRF model.

In the present study we make use of WRF/Chem version 3.1. Our set up includes the Lin et al. (1983) cloud microphysics scheme, and both wet scavenging and cloud chemistry are switched on. The Carbon Bond Mechanism extended version (CBM-Z; Zaveri et al., 1999) is used for gas-phase chemistry. The Model for Simulating Aerosol Interactions and Chemistry (MOSAIC; Zaveri et al., 2008) is chosen for simulating aerosols within eight sectional aerosol bins between 0.04 μm and 10 μm diameter. The vegetation type is

defined according to the 24-category land use data from the U. S. Geological Survey (USGS, <http://www.usgs.gov/>). As will be described in section 4, aircraft measurements of CO concentrations show no signs of anthropogenic pollution or fire emissions, indicating that these pollution types did not contribute to the low visibility observed near Iceland. To simplify our simulations, we hence ran WRF/Chem without anthropogenic emissions and without fire emissions with the intention to investigate dust and sea salt aerosols (which are produced online by the model) only. For the same reason, idealised vertical profiles as they come with the WRF/Chem software were used as initial and boundary conditions for chemical species. According to Peckham et al. (2010) idealised vertical profiles used in WRF/Chem are based upon results from the NALROM chemistry model. However, the Guenther scheme for biogenic emissions (Guenther et al., 1994) is switched on in our simulations.

WRF/Chem is run with two one-way nested grids to achieve high resolution over the flight domain. NCEP Final Analysis (FNL from GFS) 6-hourly data with 1° resolution is used for initialising meteorological conditions and as boundary conditions for the outermost domain. The NCEP data was provided by the CISL Research Data Archive through their web site at <http://dss.ucar.edu/>. The model is started on 22 February 2007 at 00 UTC.

Figure 4 shows the model domains. The first grid (G1) has a horizontal grid spacing of 20 km, the second grid (G2) 5 km and the third grid (G3) a grid spacing of 1 km. The present paper focuses on G3, which is centred on flight legs 3 to 5 to allow comparison with the aircraft measurements.

The original dust routine used in WRF/Chem together with MOSAIC has previously only been applied to regions with very different vegetation characteristics from that of Iceland (e.g. Zhao et al., 1999; Gustafson et al., 2011). The dust routine was changed here, to make WRF/Chem capable of simulating Icelandic dust storms. Furthermore, changes to the sea salt parameterisation were applied. These changes will be described in sections 3.1.1 and 3.1.2. In the following, model runs performed with the original dust and sea salt parameterisation are termed OPR, while runs using the modified parameterisation are termed MPR. Most of the results below are based on results from MPR, but some results from OPR are also shown for comparison.

3.1.1 Dust

The original dust parameterisation used together with MOSAIC is based on a wind erosion module by Shaw et al. (2008). This module calculates the total mass of wind-blown dust based on vegetation type, soil moisture and wind speed. The size distribution of dust is then retrieved by estimating the dust fraction in different size-bins based on global datasets of soil texture classes.

In OPR dust is only emitted from grid points with grassland, shrubland or savanna as vegetation type. These grid

points have a vegetation mask α (which defines the erodible fraction of a grid point) that varies between 0.055 and 0.085.

In MPR, dust is only emitted from grid points with vegetation type equal to barren or sparsely vegetated, wooded tundra, mixed tundra and bare ground tundra. To our knowledge, only very broad recommendations exist on how to choose the α values for these vegetation types. For example Nickovic et al. (2001) used an α value of 1.0 for deserts and 0.5 for semi-deserts. We therefore compared several test runs with the aircraft measurements in order to find more accurate values for Icelandic vegetation types. The best agreement with the particle measurements from the aircraft is found using $\alpha = 0.5$ for barren or sparsely vegetated, $\alpha = 0.3$ for wooded tundra, $\alpha = 0.4$ for mixed tundra and $\alpha = 0.5$ for bare ground tundra. These α values, which were chosen for MPR, can be used as a reference for future numerical modelling studies on Icelandic dust storms.

Apart from the dust and sea salt parameterisation, WRF/Chem was set up in exactly the same way for MPR and OPR. However, some rather minor deviations in simulated meteorological parameters such as temperature and wind direction occur between the two simulations. This is due to the fact that some of the parameter choices in the physical parameterisations of WRF/Chem are closely linked to the atmospheric chemistry module (Peckham et al., 2010).

Only the snow cover and ice cover included in the vegetation map from USGS are currently considered in OPR and MPR. Hence, deviations of the actual snow and ice cover for Iceland on 22 February 2007 from USGS 24 category data may cause errors in simulated dust production. A lot of clouds were present on the flight day, which precluded satellite-based derivations of detailed information on snow and ice cover for that specific day. Nonetheless, satellite images from 24 February (not shown) and 25 February (see Figure 5) revealed that large parts of South and West Iceland were indeed snow and ice free and that these areas are reasonably represented by the USGS data set. However, there is a significant underestimation of the snow and ice cover for G1 and G2. Regarding G3, the satellite images indicate that snow and ice present to the north of Mýrdalsjökull is not included in our simulations while there is an overestimation of snow and ice to the southeast of this glacier. Since the highest wind speeds occur downstream of the glacier (see Figure 7) it is assumed here that deviations from the actual snow and ice cover for G3 do not affect the dust simulations significantly. Nonetheless, it can not be ruled out that deviations from the actual snow cover in G1 and G2 may influence the dust simulations for G3 presented here.

3.1.2 Sea salt

In OPR sea salt is parameterised according to Gong and Barrie (1997). That study makes use of equation 6 from Monahan et al. (1986) to express the rate of sea salt droplet generation at the sea surface. The equation shows a monotonic

increase with decreasing particle size for diameters smaller than $0.2\ \mu\text{m}$. In contrast to this, measurements and laboratory experiments (e.g. O'Dowd and Smith, 1993; Nilsson et al., 2001; Mårtensson et al., 2003) have shown that there is a major contribution of particles in the submicrometer range with a maximum around $0.1\ \mu\text{m}$ diameter and decreasing values towards smaller sizes.

We therefore changed the sea salt parameterisation in MPR to that of Gong (2003) who introduced a modified version of the equation by Monahan et al. (1986) to reduce sea salt number flux density below $0.1\ \mu\text{m}$ and additionally increase the flux at $0.1\ \mu\text{m}$. In MPR a θ value of 11 is used for Gong's equation. According to Nilsson et al. (2007) this results in the best agreement between the simulated sea salt flux and sea salt measurements carried out at Mace Head (Ireland) between May and September 2002 for diameters between $0.01\ \mu\text{m}$ and $0.1\ \mu\text{m}$. Note that the measurements by Nilsson et al. (2007) were carried out at average water temperatures of 12°C . This implies that some errors for the simulated sea salt flux may occur due to somewhat lower water temperatures at simulation time. Laboratory simulations by Mårtensson et al. (2003) have shown that when water temperatures increase, sea salt number concentrations decrease for diameters smaller than $0.07\ \mu\text{m}$ and increase for diameters larger than $0.35\ \mu\text{m}$. Inspection of satellite images available at <http://www.remss.com> shows that the ocean had a sea surface temperature of about 8°C on the flight day.

3.2 Flexpart

The Lagrangian Particle Dispersion Model (LPDM) FLEXPART has been used to examine source regions for numerous aircraft, station, and ship-based studies (Stohl et al., 2005; Stohl, 2006; Warneke et al., 2009; Gilman et al., 2010; Hirdman et al., 2010). The model provides source information for a measurement point by examining clusters of so-called tracer particles transported in the atmosphere. Mean winds from the European Centre for Medium-Range Weather Forecasts (ECMWF, 2002) model output are included in the simulations along with parameterisations to account for turbulence and convective transport. These processes, which are not included in standard trajectory models, are important for a realistic simulation of the transport of trace substances (Stohl, 2002).

FLEXPART was run backward in time from the aircraft measurement location using operational analyses from ECMWF with $0.5^\circ\times 0.5^\circ$ resolution for FAAM flight B269. To provide releases along the flight track, 50 000 particles were released with any horizontal movement of the aircraft of 0.19° latitude or longitude, and a vertical change in pressure coordinates of 10 hPa.

The model simulation was run with a generic aerosol tracer. The aerosol tracer was removed by wet and dry deposition processes (Stohl et al., 2005). In addition, air parcels were removed from the simulation after a life-time of 20

days. Anthropogenic emissions were initialised from the updated EDGAR 3.2 emissions inventory for the year 2000 (Olivier et al., 2001).

We present the results showing a footprint 'Potential Emission Sensitivity' (PES) which represents the sensitivity of the measured air mass to global emissions backward in time for the lowest 100 m above the surface. Since most emissions occur at the surface, the footprint PES is of particular importance (Jonson, 2010).

4 Results

4.1 Aircraft measurements and WRF/Chem simulations

Measurements from 2DC and 2DP (not shown) indicate that some cloud and/or precipitation particles were present during flight legs 4 and 5, the vast majority of them inside the jet. However, only very low concentrations of less than $120\ \text{l}^{-1}$ for 2DC and not more than $0.13\ \text{l}^{-1}$ for 2DP were measured. Neither instrument detected any particles during leg 3. We deduce that errors in PCASP measurements due to clouds and precipitation are unlikely. The 2DC and 2DP measurements are mainly in agreement with locations of precipitation and clouds simulated by WRF/Chem (not shown), although some precipitation (graupel and snow) is simulated for leg 3 which is not present in the measurements.

Figure 6 shows mole fraction of CO measured at different heights by the aircraft. Values range from 145 ppb to 220 ppb, indicating that measurements were carried out in clean to moderately polluted tropospheric air away from urban areas. Typical values in clean tropospheric air range from 40 ppb to 200 ppb (Seinfeld and Pandis, 2006), while typical values in urban areas away from freeways reach 2 ppm to 10 ppm (Jacobson, 1999). The CO measurements are not correlated with PCASP particle number and mass mixing ratios which will be described below. The measurements hence show that anthropogenic pollution or fire emissions did not contribute to the low visibility observed near Iceland's south coast.

Maps of the simulated wind field and simulated mass mixing ratios at the lowest model level are shown in Figures 7 and 8, respectively. Basically, high dust mass mixing ratios are found inside the wake while values decrease towards the jet. The opposite is true for sea salt mass mixing ratio. Local wind speed maxima occur around Mýrdalsjökull, probably due to orographic effects. Large amounts of dust are produced to the north-west and south-east of the glacier. According to the Agricultural Research Institute and Soil Conservation Service of Iceland (<http://www.rala.is/desert/>), these areas suffer from considerable to extremely severe erosion. Two manned meteorological stations, one at the island Heimaey and the other located to the south of glacier Mýrdalsjökull (black stars in Figure 8 show the location

of these stations), reported poor visibility and dust on the flight day, confirming the simulations. Overall, the location of the wind speed maxima around Mýrdalsjökull relative to dust maxima indicates that orographic effects may have contributed to the formation of the dust storm. This is in agreement with Ólafsson (2005) who pointed out that local orographic effects may be important for dust storms in Iceland.

Measurements and simulations of wind speed and wind direction at all flight legs are shown in Figure 9. These two meteorological parameters are crucial for simulating dust and sea salt aerosols. Wind speed determines the amount of dust and sea salt which is brought up into the air, while wind direction constitutes the location to which aerosols are transported. Apart from some differences in wind speed at 1900 m, there is a very good agreement between the aircraft and the model. The strong increase in wind speed from the wake towards the jet measured at 400 m and 700 m height is very well captured by the model.

Corresponding results for temperature and specific humidity are shown in Figure 10. Overall the model agrees well with the aircraft. Both, observations and simulations show that temperature decreases with height. However, the static stability appears to be weaker between 400 m and 700 m in the measurements than in the simulations while the opposite is the case between 700 m and 1900 m height.

Particle mass mixing ratios and particle number concentrations are given in Figure 11. The measurements show two maxima at 400 m height, one around 20.35°W longitude (inside the wake) and one near 19.5°W longitude (inside the jet). The former one coincides with a sharp change in wind speed and wind direction (see Figure 9). Convergence of air masses may be an explanation for the formation of this peak. The results shown in Figure 8 (note that the location of the two measured mass mixing ratio peaks is given by the black triangles) indicate that the latter peak is caused by dust transported from sand fields located to the south-east of the Mýrdalsjökull glacier towards the ocean, while the former one can be associated with dust sources to the west of this glacier. Figure 11 shows that the measured particle mass mixing ratios and particle number concentrations generally decrease as the aircraft flies away from Iceland towards the jet.

Simulations for the sum of all aerosol types represented by the model (red line in Figure 11) catch the shape of measured mass mixing ratios and particle concentrations well. However, the location of the western peak is simulated further north-westwards than the corresponding measured peak. There is also some disagreement concerning the magnitude of the values with a tendency for WRF/Chem to overestimate dust inside the wake and to underestimate sea salt inside the jet.

Comparing simulations at 400 m height for dust and sea salt with the sum of all aerosol types represented by the model indicates that the high particle mixing ratios and particle number concentrations measured inside the wake and in

the north-western part of the jet west of 19.5°W are due to dust. Sea salt aerosols become the dominating aerosol type as the aircraft flies away from Iceland towards the jet. This is in agreement with air mass source regions identified by Flexpart which will be described in section 4.2.

Total scattering coefficients measured by a nephelometer at 750 nm, 550 nm and 450 nm wavelength on board the FAAM aircraft show the same features as the particle mass mixing ratios, i.e. an overall decrease from the wake towards the jet and a two peak pattern, and are therefore not shown here. At 700 nm wavelength and at 400 m height, values of up to $8 \times 10^{-4} \text{ m}^{-1}$ were reached at the location of the two maxima in particle mass mixing ratio.

Measured mass mixing ratio and particle number concentration do not change significantly from 400 m to 700 m height. However, the two peaks measured at 700 m are poorly simulated by the model. This could be due to less vertical mixing and more stable conditions between 400 m and 700 m height in the simulations than in the observations (see discussion of Figure 10, above).

At 1900 m, the particle mass mixing ratio is close to zero and only values of about $20 \mu\text{g}/\text{kg}$ are found inside the jet. This is well represented by the model. In contrast to this, particle number concentration is poorly simulated at this height, with the measurements showing a peak at 18.9°W longitude inside the jet, while simulations show a peak inside the wake region.

Further inspection of the model results shows, that the simulated peak in particle number concentration is due to sulfate and organic carbon which dominate at this flight level. This is in contrast to simulations of particle number concentrations at lower heights and in contrast to particle mass mixing ratio at all flight levels (including the highest one), which are all strongly dominated by dust and sea salt aerosols. Simulated sulfate and organic carbon seem to originate from volcano emissions used to initialise the model and from biogenic emissions (calculated online and possibly also included in the initial conditions), respectively. As described earlier in this section, some precipitation (graupe and snow) is simulated for leg 3 which is not present in the 2DC and 2DP measurements. Therefore, unrealistic washout may contribute to the simulated decrease in particle concentration towards the jet. However, this decrease can also be partly explained by the increasing distance to land sources of sulfate and organic carbon towards the jet.

The peak at 18.9°W longitude in particle number concentration measured by PCASP is not present in the corresponding mass mixing ratio measurements. This indicates that the peak is caused by particles which are lighter and therefore smaller than sea salt and dust aerosols. It could be due to volcanic emissions or sulfate produced from DMS not included in the model set up. A contribution from anthropogenic sources or wildfires is very unlikely since the CO measurements described above are typical for a clean to moderately polluted atmospheric background profile carried

out away from urban areas and do not show a peak at this location. The fact that simulations of particle number agree much better with PCASP for the lower flight legs than for the one at 1900 m height indicates that upper air mass properties differ from the air mass properties at lower flight legs.

OPR significantly underestimates the magnitude of particle mass mixing ratios and particle number concentrations (see Figure 12). However, the main features of the measurements, i.e. a decrease in particle mass mixing ratio and particle number concentration from the wake towards the jet, are caught. The two peak pattern measured by the aircraft at 400 m and 700 m height is not present in OPR.

Overall, changes applied to the dust and sea salt parameterisation in MPR have substantially improved the simulations of dust and sea salt aerosols near Iceland. However, uncertainties remain in MPR associated with the snow cover (especially for G1 and G2), assumptions made in dust and sea salt parameterisations and contributions from emission sources neglected by our model set up.

4.2 Flexpart simulations

Figure 13 shows PES for the aerosol tracer for flight legs 5 and 3. Results for flight leg 4 are very similar to flight leg 5 and are therefore not shown here. Simulations were started on 22 February at 11:57 UTC and 10:53 UTC for leg 5 and 3, respectively. These are times when the aircraft was located inside the wake. The plume centroid locations, derived from a statistical cluster analysis (see Stohl et al. (2005) and Stohl et al. (2002)), for up to 6 days backward in time are represented by black circles. The centroids can be regarded as a trajectory back from the measurement location, if a plume does not split significantly.

At 400 m height (Figure 13 (a)), PES shows the highest values in the northeasterly flow over South Iceland. There is high sensitivity over Icelandic dust emission source regions. Centroid locations suggest that the air masses investigated by the aircraft originated from Scandinavia two to five days ahead of the flight day, but were then transported over the Norwegian Sea towards Iceland.

For flight leg 3 (Figure 13 (b)), centroids take a clockwise track backward in time from Iceland towards Greenland. The PES in the cyclonic flow to the south of Iceland is higher compared to Flexpart simulations for flight leg 5.

Note that Flexpart simulations were also carried out for times when the aircraft was located inside the jet (not shown). These simulations indicate that the air was of much more maritime origin for measurements carried out inside the jet, which is in agreement with the WRF/Chem results (see section 4.1). Apart from this, the results basically show the same as for times when the aircraft was located inside the wake.

Overall, Flexpart simulations suggest significantly different air mass histories for the 1900 m flight leg and the lower elevation legs. In agreement with the conclusion drawn in section 4.1, this could explain why WRF/Chem performs

much better in simulating particles at lower flight legs than at flight leg 3. Particles detected at lower flight legs are most likely purely Icelandic dust and sea salt aerosols, while other (most likely natural) emission sources may have contributed to the particle concentration measured at 1900 m height.

5 CALIPSO observations

Although simulations presented here focus on the flight day, wind data from the QuikSCAT satellite (not shown) reveal that comparable wind speed conditions (i.e. wind speeds of more than 20 m/s and a barrier jet and wake pattern) were already present on 20 February and lasted until approximately 23 February. This implies that the dust storm may already have developed some time before the flight was carried out. In fact, the meteorological station at Heimaey also reported dust for the morning of 21 February. There is further evidence from the Cloud Aerosol Lidar with Orthogonal Polarization (CALIOP) on board the Cloud-Aerosol Lidar Infrared Pathfinder Satellite Observation (CALIPSO) satellite that dust and marine aerosols were present on 21 February near Iceland's south coast. However, CALIPSO also detected a lot of dust and polluted dust over the north-western Icelandic land surface. The latter seems to be very unlikely, since other satellite images (e.g. Figure 5) show that this part of Iceland was covered by snow. Hence, we do not present CALIPSO results here, due to concerns about the reliability of the data. Information on uncertainties associated with CALIPSO version 3.01 products (which were investigated here) is given by Kacenelenbogen et al. (2011).

6 Summary and conclusions

A dust storm near Iceland which occurred in a barrier jet event during GFDex has been investigated based on aircraft observations and the mesoscale model WRF/Chem. The results document the transport of dust from Icelandic sand fields towards the ocean, thereby reducing visibility near Iceland's south coast significantly.

Changes have been applied to the dust and sea-salt parameterisations to make WRF/Chem capable of simulating Icelandic dust storms. A good agreement between measurements and simulations has been achieved. However, some disagreement between measurements and simulations remains concerning the magnitude of the values, with a tendency for WRF/Chem to overestimate dust and to underestimate sea salt. The simulations could be improved by including the most up to date information on snow cover in the dust parameterisation and by further optimisation of the dust and sea salt parameterisations. Inclusion of data from a global chemical transport model for initial and boundary conditions and other emission sources not taken into account in our model set up could further improve the simulations, especially for the upper flight leg at 1900 m height.

The location of local wind speed maxima relative to dust maxima indicates that orographic effects may have contributed to the formation of the dust storm. Results presented here highlight the usefulness of a high resolution model for simulating Icelandic dust storms, which is in agreement with Ólafsson (2005). Local wind speed maxima associated with orography will most likely not be adequately represented by global climate models. Assuming that orographic effects contribute to the majority of Icelandic dust storms, these effects should be parameterised in global climate models. Moreover, Icelandic dust storms in a warmer climate should be investigated in future studies. Icelandic glaciers have been retreating in recent decades. Since this trend is expected to continue with global warming, Icelandic dust activity may increase in the future (Prospero et al., 2008; Prospero et al., 2012).

Iceland is an important global source of dust with deposition rates comparable to or higher than those found for other areas that are usually considered to contribute to major global dust emissions (Arnalds, 2010; Prospero et al., 2012). In agreement with the results of the present study, Ovadnevaite et al. (2009) showed that dust outbreaks from Iceland can increase levels of absorbing material and light scattering over the North Atlantic. Ovadnevaite et al. (2009) concluded that dust from Icelandic sand fields may be a significant regional source of aerosols over the North Atlantic and hence should be considered in regional and global climate models. Future studies are required to determine the impacts of an inadequate representation of Icelandic dust sources in climate simulations.

To our knowledge, apart from the record by Prospero et al. (2012), no comprehensive data set describing the frequency of Icelandic dust storms exists. Although in-situ data have been used together with visible satellite imagery from passive remote sensors (e.g. Ovadnevaite et al., 2009; Arnalds, 2010; Prospero et al., 2012) to verify the transport of dust from Iceland towards the ocean, this method is only successful for dust storms which are not hidden by clouds. Active remote sensors like CALIOP on board CALIPSO can look through clouds to some extent, but their poor spatial coverage would prohibit the derivation of a meaningful climatology. This means that a combined approach, using numerical models, satellites and measurements is required to derive statistics about Icelandic dust storms.

Overall, the modelling approach presented here constitutes a promising basis to investigate important questions on Icelandic dust storms addressed in this section.

Acknowledgements. This work was funded by the Norwegian Research Council through the POLARCAT project, project no. 175916. The corresponding author is currently funded by the Natural Environment Research Council (NERC) through its National Centre for Atmospheric Science (NCAS). Thanks to the British Atmospheric Data Centre (BADC), which is part of NCAS, for providing the GFDex data on their web page. We also thank the people behind the CISL Research Data Archive for

providing NCEP data on their web site. Thanks to the European Centre for Medium-Range Weather Forecasts (ECMWF) and the Norwegian Meteorological Institute for providing access to ECMWF data. CALIPSO data were obtained from the NASA (National Aeronautics and Space Administration) Langley Research Center Atmospheric Science Data Center. MODIS images were received from the NASA/GSFC Rapid Response system (<http://lance.nasa.gov/imagery/rapid-response/>). SST images from www.remss.com are produced by Remote Sensing Systems and sponsored by National Oceanographic Partnership Program (NOPP), the NASA Earth Science Physical Oceanography Program, and the NASA MEaSUREs DISCOVER Project. QuikSCAT data were obtained from the Physical Oceanography Distributed Active Archive Center (PO.DAAC) at the NASA Jet Propulsion Laboratory, Pasadena, California (<http://podaac.jpl.nasa.gov>).

References

- Arnalds, O.: The Icelandic 'rofabard' soil erosion features, *Earth Surf. Process. Landforms*, 25, 17–28, 2000.
- Arnalds O.: Dust sources and deposition of aeolian materials in Iceland, *Icel. Agric. Sci.*, 23, 3–21, 2010.
- Arnalds, O., Gísladóttir, F. O., and Sigurjónsson, H.: Sandy deserts of Iceland: an overview, *J. Arid Environ.*, 47, 359–371, 2001.
- Crochet, P., Jóhannesson, T., Jónsson, T., Sigurdsson, O., Björnsson, H., Pálsson, F. and Barstad, I.: Estimating the spatial distribution of precipitation in Iceland using a linear model of orographic precipitation, *J. of Hydrometeorol.*, 8(6), 1285–1306, 2007.
- ECMWF: IFS Documentation, edited by White, P. W., ECMWF, Reading, UK, 2002.
- Gilman, J. B., Burkhart, J. F., Lerner, B. M., Williams, E. J., Kuster, W. C., Goldan, P. D., Murphy, P. C., Warneke, C., Fowler, C., Montzka, S. A., Miller, B. R., Miller, L., Oltmans, S. J., Ryerson, T. B., Cooper, O. R., Stohl, A., and de Gouw, J. A.: Ozone variability and halogen oxidation within the Arctic and sub-Arctic springtime boundary layer, *Atmos. Chem. Phys.*, 10, 10223–10236, doi:10.5194/acp-10-10223-2010, 2010.
- Gong, S. L., and Barrie, L. A.: Modeling sea-salt aerosols in the atmosphere - 1. Model development, *J. Geophys. Res.*, 102, 3805–3818, doi:10.1029/96JD02953, 1997.
- Gong, S. L.: A parameterization of sea-salt aerosol source function for sub- and super-micron particles, *Global Biogeochem. Cy.*, 17, 4, 1097, doi:10.1029/2003GB002079, 2003.
- Grell, G. A., Peckham, S. E., Schmitz, R., McKeen, S. A., Frost, G., Skamarock, W. C., and Eder, B.: Fully coupled 'online' chemistry within the WRF model, *Atmos. Environ.*, 39, 6957–6976, doi:10.1016/j.atmosenv.2005.04.027, 2005.
- Guenther, A., Zimmerman, P., and Wildermuth, M.: Natural volatile organic compound emission rate estimates for US woodland landscapes, *Atmos. Environ.*, 28, 1197–1210, 1994.
- Gustafson, W. I., Jr., Qian, Y. and Fast, J. D.: Downscaling Aerosols and the Impact of Neglected Subgrid Processes on Direct Aerosol Radiative Forcing for a Representative Global Climate Model Grid Spacing, *J. Geophys. Res.*, 116, D13303, doi:10.1029/2010JD015480, 2011.
- Hirdman, D., Burkhart, J. F., Sodemann, H., Eckhardt, S., Jefferson, A., Quinn, P. K., Sharma, S., Strom, J., and Stohl, A.: Long-term trends of black carbon and sulphate aerosol in the Arctic:

- changes in atmospheric transport and source region emissions, *Atmos. Chem. Phys.*, 10, 9351–9368, doi:10.5194/acp-10-9351-2010, 2010.
- Ingólfsson, Ó.: The dynamic climate of Iceland, http://www3.hi.is/oi/climate_in_iceland.htm, accessed 16.01.2012, 2008.
- Jacobson, M. Z.: *Fundamentals of atmospheric modelling*, Cambridge University Press, 1999.
- Jonson, J. E., Stohl, A., Fiore, A. M., Hess, P., Szopa, S., Wild, O., Zeng, G., Dentener, F. J., Lupu, A., Schultz, M. G., Duncan, B. N., Sudo, K., Wind, P., Schulz, M., Marmer, E., Cuvelier, C., Keating, T., Zuber, A., Valdebenito, A., Dorokhov, V., De Backer, H., Davies, J., Chen, G. H., Johnson, B., Tarasick, D. W., Stbi, R., Newchurch, M. J., von der Gathen, P., Steinbrecht, W., and Claude, H.: A multi-model analysis of vertical ozone profiles, *Atmos. Chem. Phys.*, 10, 5759–5783, doi:10.5194/acp-10-5759-2010, 2010.
- Kacenelenbogen, M., Vaughan, M. A., Redemann, J., Hoff, R. M., Rogers, R. R., Ferrare, R. A., Russell, P. B., Hostetler, C. A., Hair, J. W., and Holben, B. N.: An accuracy assessment of the CALIOP/CALIPSO version 2/version 3 daytime aerosol extinction product based on a detailed multi-sensor, multi-platform case study, *Atmos. Chem. Phys.*, 11, 3981–4000, doi:10.5194/acp-11-3981-2011, 2011.
- Lin, Y.-L., Farley, R. D., and Orville, H. D.: Bulk parameterization of the snow field in a cloud model, *J. Climate Appl. Meteor.*, 22, 1065–1092, 1983.
- Mårtensson, E. M., Nilsson, E. D., de Leeuw, G., Cohen, L. H., and Hansson, H.-C.: Laboratory simulations and parameterization of the primary marine aerosol production, *J. Geophys. Res.*, 108(D9), 4297, doi:10.1029/2002JD002263, 2003.
- Monahan, E. C., Spiel, D. E., and Davidson, K. L.: A model of marine aerosol generation via whitecaps and wave disruption, in *Oceanic Whitecaps*, edited by E. C. Monahan and G. Mac-Niochaill, pp. 167–193, D. Reidel, Norwell, Mass., 1986.
- Nickovic, S., Kallos, G., Papadopoulos, A., and Kakaliagou, O.: A model for prediction of desert dust cycle in the atmosphere, *J. Geophys. Res.*, 106, 18113–18129, 2001.
- Nilsson, E. D., Rannik, U., Swietlicki, E., Leek, C., Aalto, P. P., Zhou, J. and Norman, M.: Turbulent aerosol fluxes over the Arctic Ocean 2. Wind-driven sources from the sea, *J. Geophys. Res.*, 106, 32139–32154, doi:10.1029/2000JD900747, 2001.
- Nilsson, E. D., Mårtensson, E. M., Van Ekeren, J. S., de Leeuw, G., Moerman, M., and O'Dowd, C.: Primary marine aerosol emissions: size resolved eddy covariance measurements with estimates of the sea salt and organic carbon fractions, *Atmos. Chem. Phys. Discuss.*, 7, 13345–13400, doi:10.5194/acpd-7-13345-2007, 2007.
- O'Dowd, C. D., and Smith, M. H.: Physiochemical properties of aerosols over the northeast Atlantic: Evidence for wind-related submicron sea-salt aerosol production, *J. Geophys. Res.*, 98(D1), 1137–1149, doi:10.1029/92JD02302, 1993.
- Ólafsson, H., Petersen, G. N., Renfrew, I., Kristjánsson, J. E., and Moore, G. W.: The South-Iceland wake, manuscript in preparation.
- Ólafsson, H.: Multi-scale orographic forcing of the atmosphere leading to an erosion event, *Proceedings of the 28th International Conference on Alpine Meteorology (ICAM) and the Annual Scientific Meeting of the Mesoscale Alpine Programme (MAP)*, Zadar, Croatia, 2005.
- Olivier, J. G. J. and Berdowski, J. J. M.: Global emissions sources and sinks, *The Climate System*, edited by: Berdowski, J., Guicherit, R., and Heij, B. J., A. A. Balkema Publishers/Swets and Zeitlinger Publishers, Lisse, The Netherlands, 33–78, 2001.
- Ovadnevaite, J., Ceburnisa, D., Plauskaite-Sukienė, K., Modin, R., Dupuy, R., Rimselyte, I., Ramonet, M., Kvitkusb, K., Ristovski, Z., Berresheima, H. and O'Dowd, C. D.: Volcanic sulphate and arctic dust plumes over the North Atlantic Ocean, *Atmos. Environ.*, 43, 4968–4974, doi:10.1016/j.atmosenv.2009.07.007, 2009.
- Peckham, S. E., Grell, G. A., McKeen, S. A., Fast, J. D., Gustafson, W. I., Ghan, S. J., Zaveri, R., Easter, R. C., Barnard, J., Chapman, E., Wiedinmyer, C., Schmitz, R., Salzmann, M. and Freitas, S. R.: *WRF/Chem Version 3.2 User's Guide*, 2010.
- Prospero, J. M., Arnalds, Ó., Ólafsson, H., Bullard, J. E., and Hodgkins, R.: Iceland dust storms linked to glacial outwash deposits and to sub-glacial flood (Jökulhlaup) events, *AGU Fall Meeting 2008*, San Francisco, USA, A13E-08, 2008.
- Prospero, J. M., Bullard, J. E., and Hodgkins, R.: High-Latitude Dust Over the North Atlantic: Inputs from Icelandic Proglacial Dust Storms, *Science*, 335, 1078–1082, 2012.
- Renfrew, I. A., Moore, G. W. K., Kristjánsson, J. E., Ólafsson, H., Gray, S. L., Petersen, G. N., Bovis, K., Brown, P., Fore, I., Haine, T. W. N., Hay, C., Irvine, E. A., Oghuishi, T., Outten, S. D., Pickart, R., Shapiro, M. A., Sproson, D., Swinbank, R., Wooley, A., and Zhang, S.: The Greenland Flow Distortion experiment. *Bull. Am. Meteorol. Soc.*, 88, 1307–1324, 2008.
- Rögnvaldsson, Ó., Jónsdóttir, J. F. and Ólafsson, H.: Numerical simulations of precipitation in the complex terrain of Iceland-comparison with glaciological and hydrological data, *Meteorol. Z.* 16(1), 71–85, 2007.
- Schumann, U., Weinzierl, B., Reitebuch, O., Schlager, H., Minikin, A., Forster, C., Baumann, R., Sailer, T., Graf, K., Mannstein, H., Voigt, C., Rahm, S., Simmet, R., Scheibe, M., Lichtenstern, M., Stock, P., Rba, H., Schuble, D., Tafferner, A., Rautenhaus, M., Gerz, T., Ziereis, H., Krautstrunk, M., Mallaun, C., Gayet, J.-F., Lieke, K., Kandler, K., Ebert, M., Weinbruch, S., Stohl, A., Gasteiger, J., Gro, S., Freudenthaler, V., Wiegner, M., Ansmann, A., Tesche, M., Ólafsson, H., and Sturm, K.: Airborne observations of the Eyjafjalla volcano ash cloud over Europe during air space closure in April and May 2010, *Atmos. Chem. Phys.*, 11, 2245–2279, doi:10.5194/acp-11-2245-2011, 2011.
- Seinfeld, J. H. and Pandis, S. P.: *Atmospheric Chemistry and Physics - From Air Pollution to Climate Change (2nd Edition)*, John Wiley and Sons, 2006.
- Shaw, J. S., Allwine, K. J., Fritz, B. G., Rutz, F. C., Rishel, J. P., and Chapman, E. G.: An evaluation of the wind erosion module in DUSTAN, *Atmos. Environ.*, 42, 1907–1921, doi:10.1016/j.atmosenv.2007.11.022, 2008.
- Skamarock, W. C., Klemp, J. B., Dudhia, J., Gill, D. O., Barker, D. M., Duda, M., Huang, X.-Y., Wang, W. and Powers, J. G.: A Description of the Advanced Research WRF Version 3, NCAR Technical note NCAR/TN-475+STR, 2008.
- Stohl, A.: On the pathways and timescales of intercontinental air pollution transport, *J. Geophys. Res.*, 107(D23), 4684, doi:10.1029/2001JD001396, 2002.
- Stohl, A.: Characteristics of atmospheric transport into the Arctic troposphere, *J. Geophys. Res.*, 111, D11306, 2006.

doi:10.1029/2005JD006888, 2006.

Stohl, A., S. Eckhardt, C. Forster, P. James, N. Spichtinger, and Seibert, P.: A replacement for simple back trajectory calculations in the interpretation of atmospheric trace substance measurements, *Atmos. Environ.*, 36, 4635–4648, 2002.

Stohl, A., Forster, C., Frank, A., Seibert, P. and Wotawa, G.: Technical note: The Lagrangian particle dispersion model, *Atmos. Chem. Phys.*, 5, 2461–2474, 2005.

Taylor, J. P., Glew, M. D., Coakley, J. A., Tahnk, W. R., Platnick, S., V. Hobbs, P., and Ferek, R. J.: Effects of Aerosols on the Radiative Properties of Clouds. *J. Atmos. Sci.*, 57, 2656–2670, 2000.

Thorsteinsson, T., Gísladóttir, G., Bullard, J., and McTainsh, G.: Dust storm contributions to airborne particulate matter in Reykjavík, Iceland, *Atmos. Environ.*, doi:10.1016/j.atmosenv.2011.05.023, 2011, in press.

Warneke, C., Bahreini, R., Brioude, J., Brock, C. A., de Gouw, J. A., Fahey, D. W., Froyd, K. D., Holloway, J. S., Middlebrook, A., Miller, L., Montzka, S., Murphy, D. M., Peischl, J., Ryerson, T. B., Schwarz, J. P., Spackman, J. R., and Veres, P.: Biomass burning in Siberia and Kazakhstan as an important source for haze over the Alaskan Arctic in April 2008, *Geophys. Res. Lett.*, 36, L02813, doi:10.1029/2008GL036194, 2009.

Zaveri, R. A., Easter, R. C., Fast, J. D. and Peters, L. K.: Model for Simulating Aerosol Interactions and Chemistry (MOSAIC), *J. Geophys. Res.*, 113, D13204, doi:10.1029/2007JD008792, 2008.

Zaveri, R. A., and Peters, L. K.: A new lumped structure photochemical mechanism for large-scale applications, *J. Geophys. Res.*, 104(D23), 387–30, 415, doi:10.1029/1999JD900876, 1999.

Zhao, C., Liu, X., Leung, L. R., Johnson, B., McFarlane, S. A., Gustafson Jr., W. I., Fast, J. D., and Easter, R.: The spatial distribution of mineral dust and its shortwave radiative forcing over North Africa: modeling sensitivities to dust emissions and aerosol size treatments, *Atmos. Chem. Phys.*, 10, 8821–8838, doi:10.5194/acp-10-8821-2010, 2010.

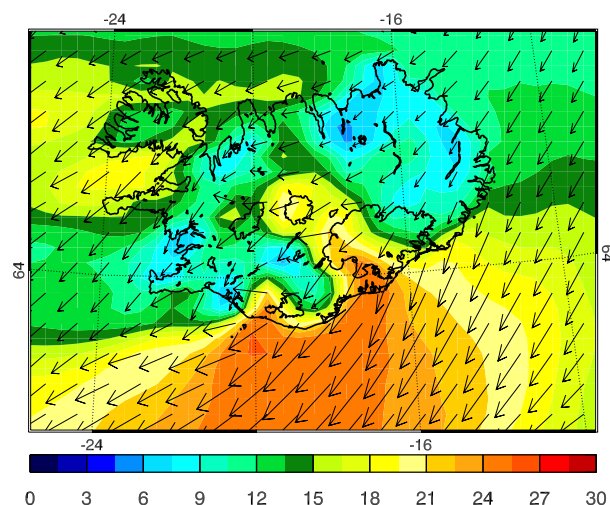


Fig. 1. Wind speed [m/s] (colored shadings) and wind direction (black arrows) from the WRF/Chem simulation at the lowest model level for G1 on 22 February 12 UTC (see section 3.1 for a description of the model configuration).

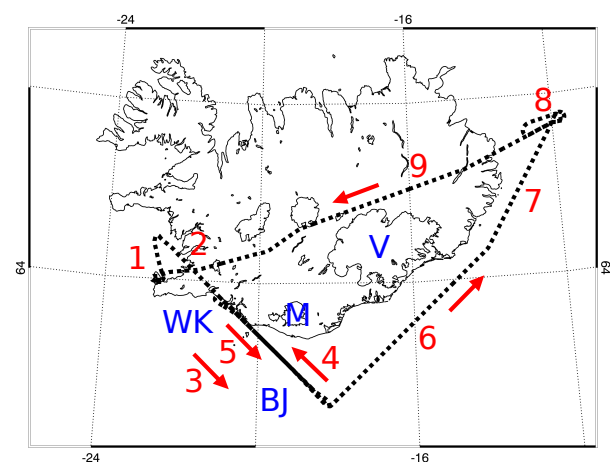


Fig. 2. Aircraft track (dotted line) for flight B269 of the GFDex campaign. The red numbers correspond to different flight legs: (1) take-off, (2) ascending, (3) at 1900 m, (4) at 700 m, (5) at 400 m, (6) ascending, (7–9) at 7600 m. The location of the wake jet, barrier jet, Mýrdalsjökull glacier and Vatnajökull glacier are indicated by WK, BJ, M and V respectively. The glaciers are also shown by land contours.

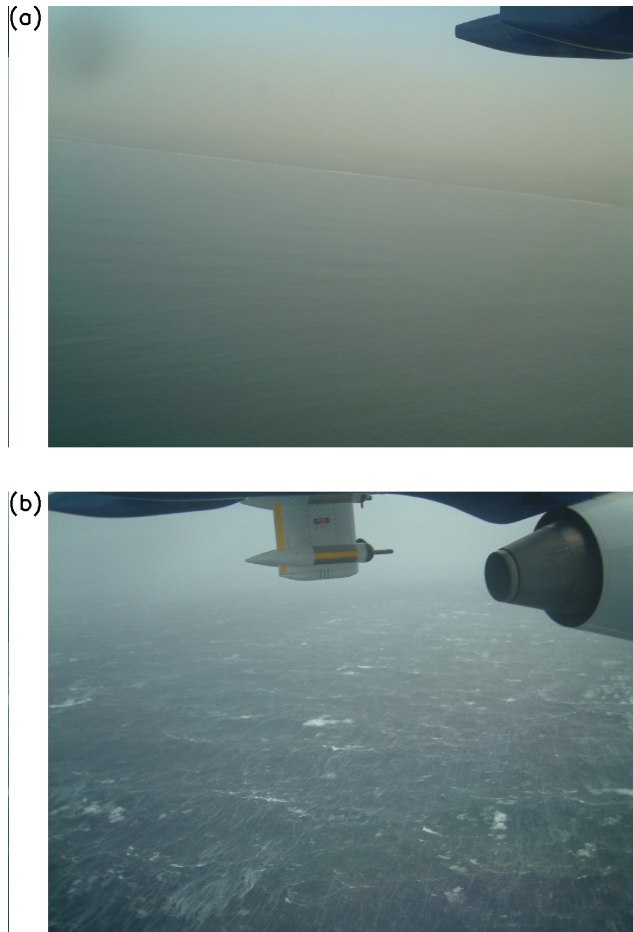


Fig. 3. Photos taken aboard the aircraft showing (a) dust in the wake and (b) the rough sea-surface in the jet.

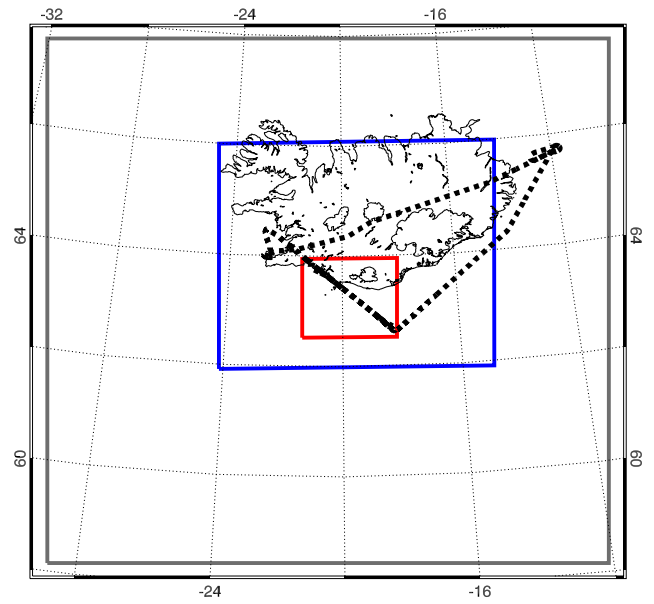


Fig. 4. The WRF/Chem model domains. The grey box shows G1, the blue box G2 and the red box G3. The dotted line corresponds to the aircraft track.

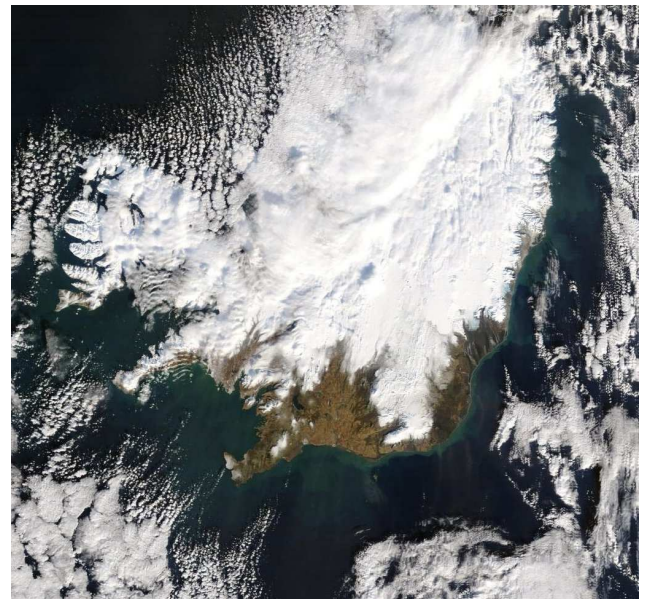


Fig. 5. MODIS Terra true-color satellite image from 25 February 2007 at 13:20 UTC (image courtesy of the NASA/GSFC Rapid Response system, <http://lance.nasa.gov/imagery/rapid-response/>).

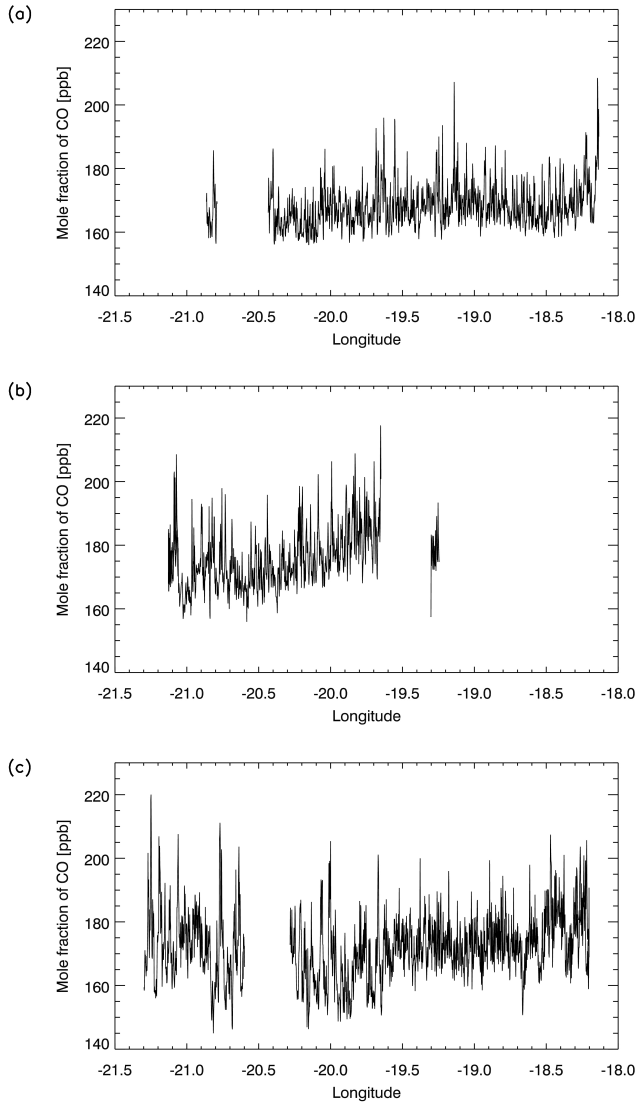


Fig. 6. Aircraft measurements of mole fraction of CO [ppb] for (a) 400 m height, (b) 700 m height and (c) 1900 m height.

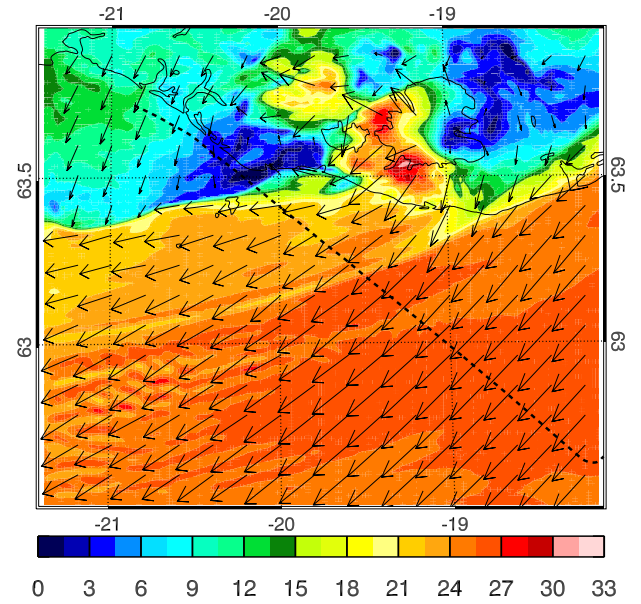


Fig. 7. Simulated wind speed [m/s] (colored shadings) and wind direction (black arrows) at the lowest model level for G3 on 22 February 12 UTC. The dotted line corresponds to leg 5 (400 m height) of the aircraft track. The thin black contours represent land contours.

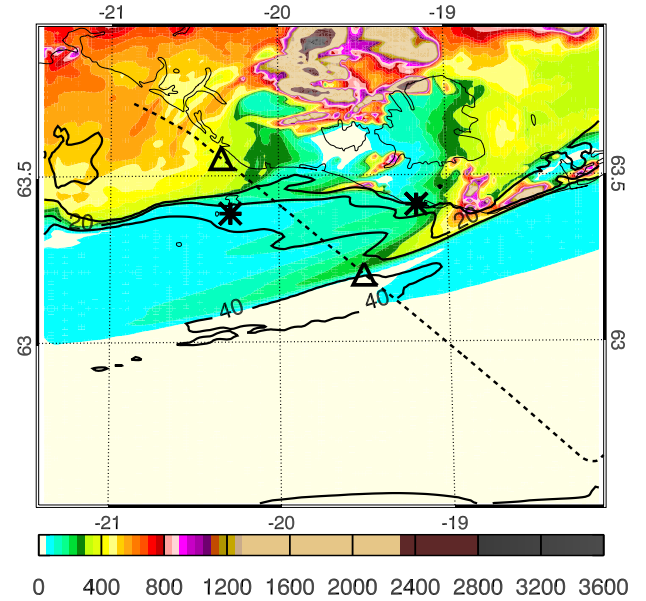


Fig. 8. As in Figure 7 but for dust mass mixing ratio [$\mu\text{g}/\text{kg}$] (colored shadings) and sea salt mass mixing ratio [$\mu\text{g}/\text{kg}$] (thick black contours) for particle diameters between $0.04 \mu\text{m}$ and $10 \mu\text{m}$. Locations of the two mass mixing ratio peaks measured at 400 m (see Figure 11) are indicated by black triangles. The black stars show locations of two manned weather stations which reported dust on the flight day.

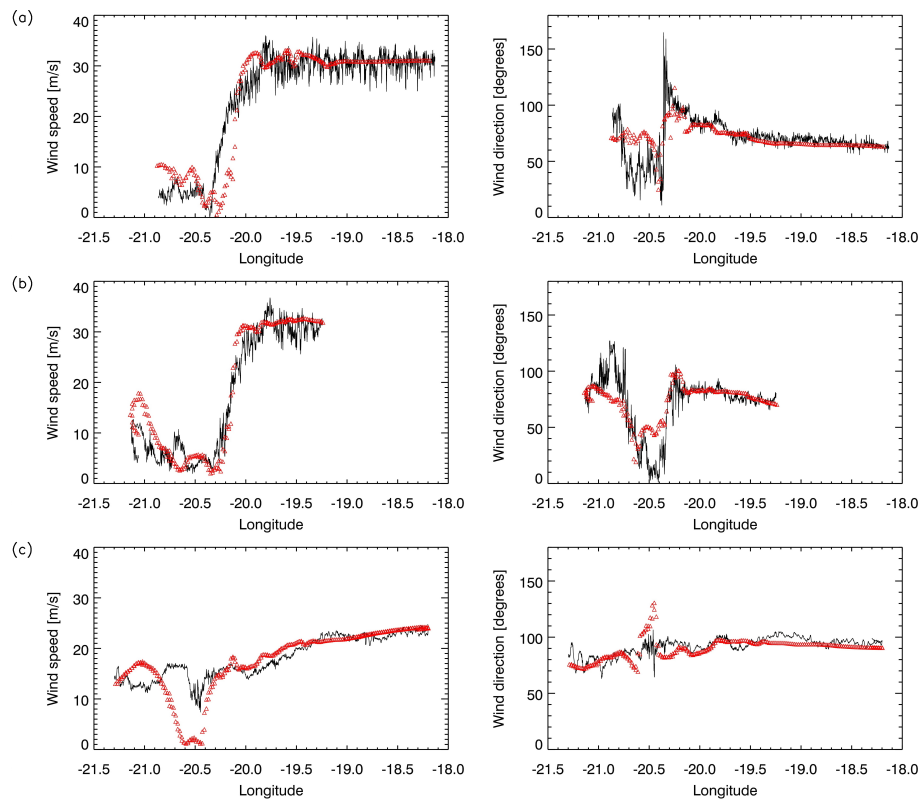


Fig. 9. Aircraft measurements (black lines) and G3 simulations from the run MPR (red triangles) at (a) 400 m height, (b) 700 m height and (c) 1900 m height. Wind speed [m/s] is shown by panels on the left and wind direction [degrees] by panels on the right.

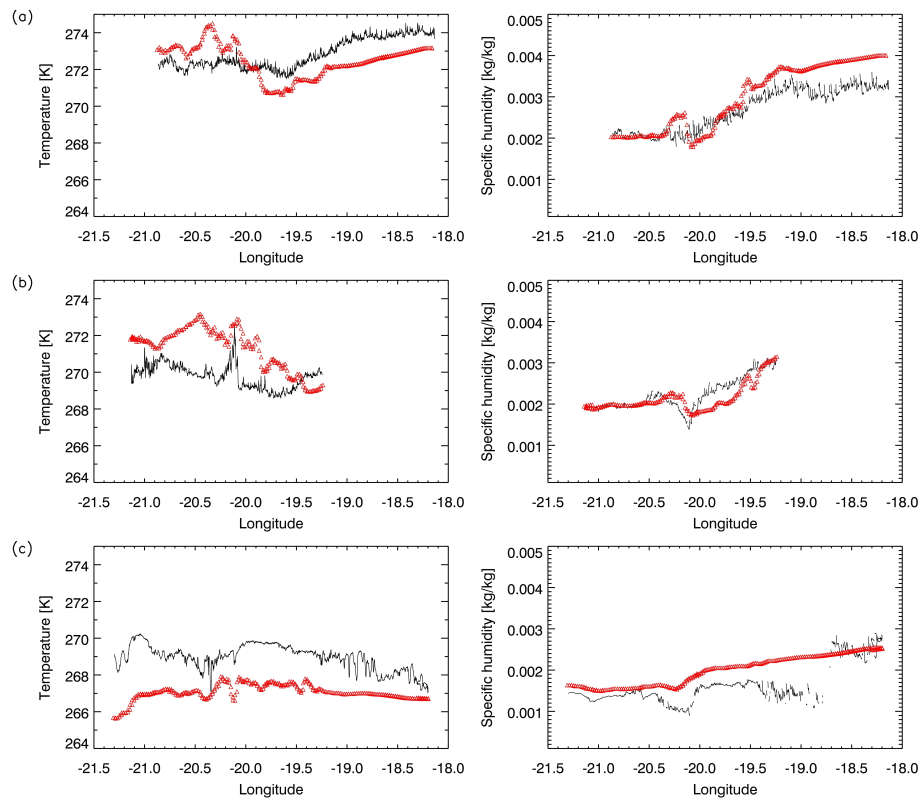


Fig. 10. As in Figure 9 but for temperature [K] (panels on the left) and specific humidity [kg/kg] (panels on the right).

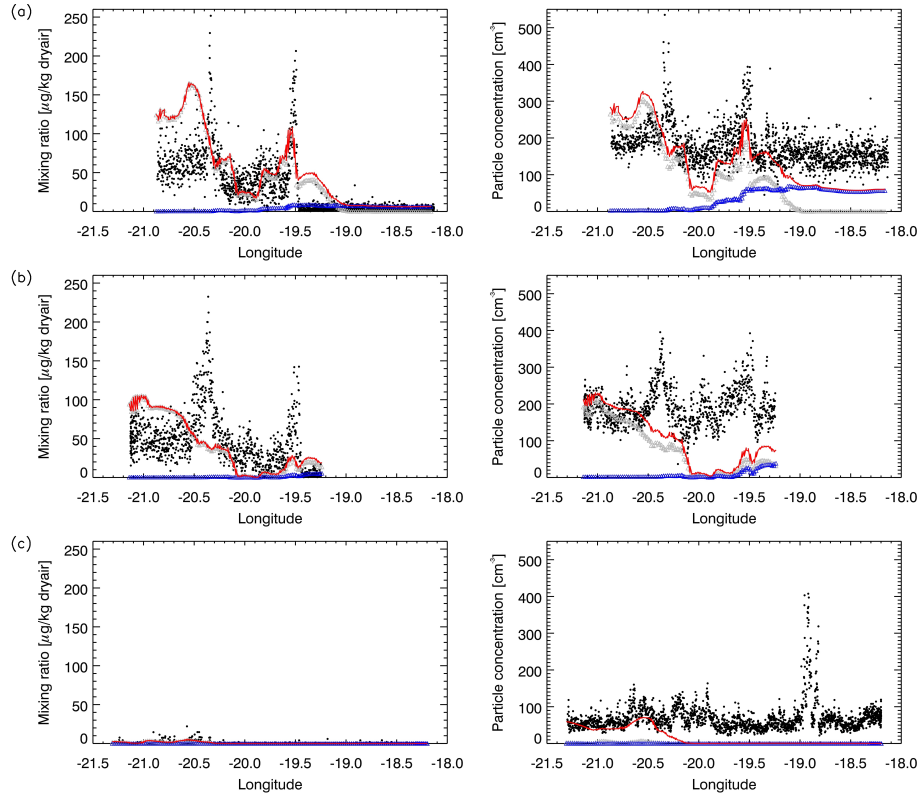


Fig. 11. As in Figure 9 but for particle mass mixing ratio [$\mu\text{g}/\text{kg}$] (panels on the left) and particle number concentration [cm^{-3}] (panels on the right). The black dots correspond to aircraft measurements from PCASP. The red line shows the sum of all simulated aerosol types (i.e. dust, sea salt, black carbon, organic carbon, ammonium, nitrate and sulfate). Grey triangles show simulated dust and blue triangles simulated sea salt. Model results are only shown for diameters between $0.1\ \mu\text{m}$ and $3.0\ \mu\text{m}$ to allow comparison to the PCASP measurements.

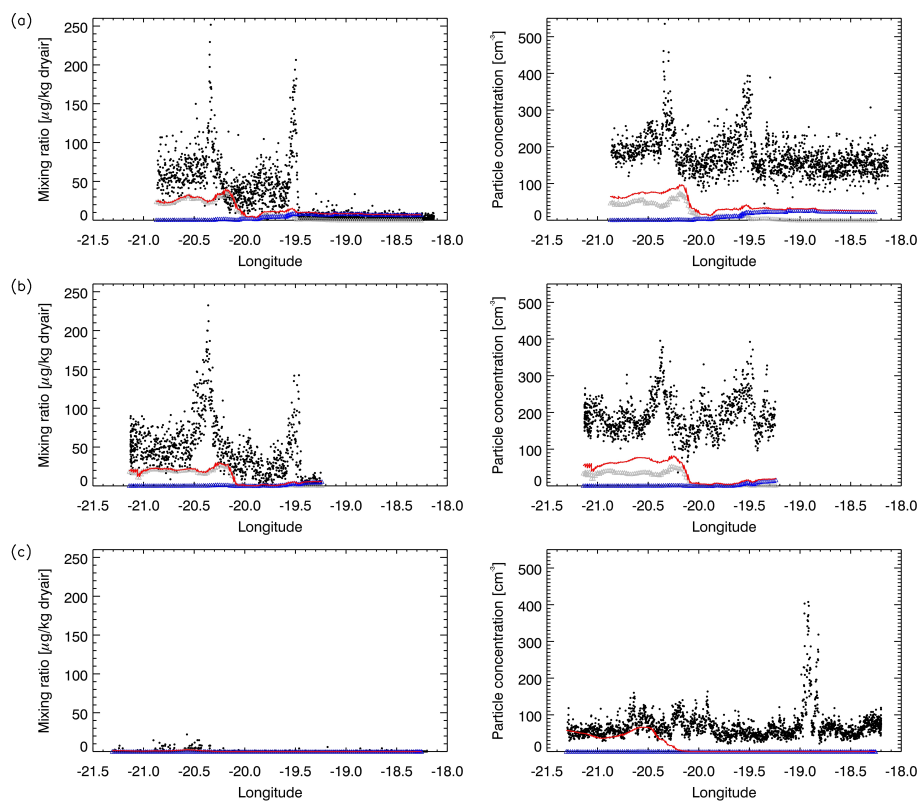


Fig. 12. As in Figure 11 but for model results from the run OPR.

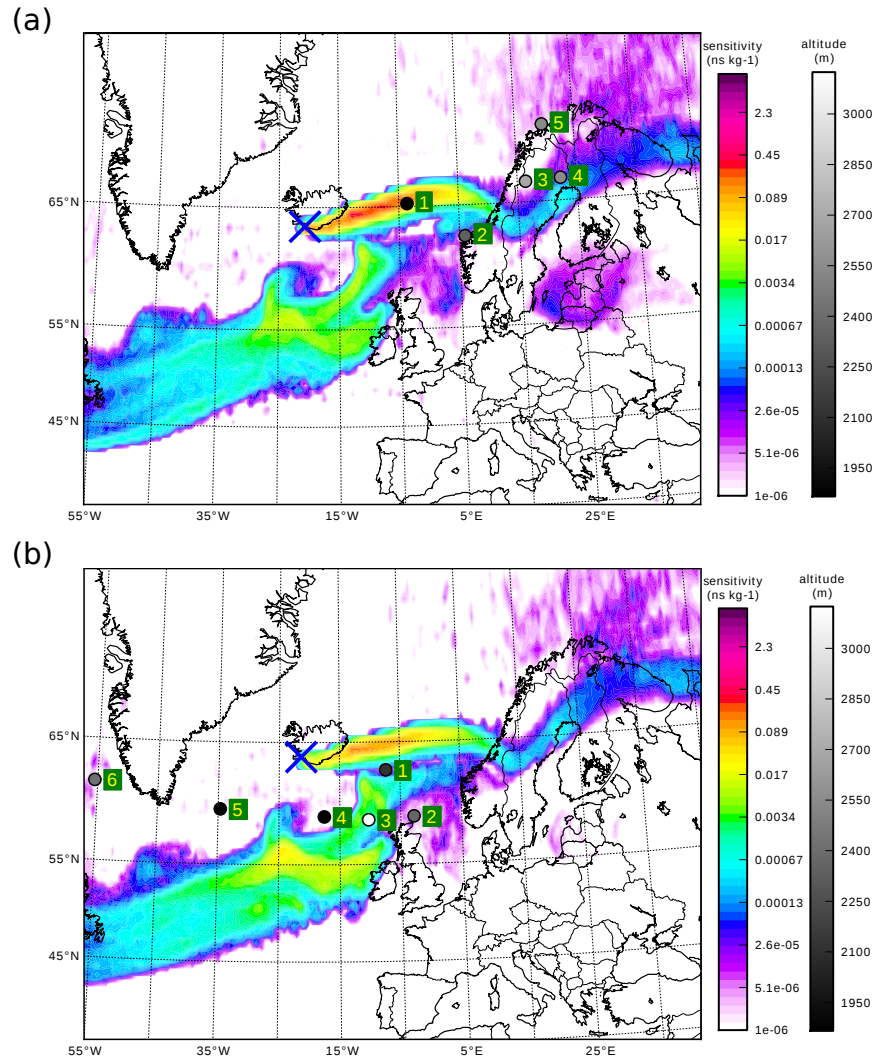


Fig. 13. Flexpart aerosol tracer footprint PES [ns/kg] (colored shadings) for (a) flight leg 5 (400 m height) and (b) flight leg 3 (1900 m height). Black circles represent plume centroid locations for a specific day back in time (see yellow numbers inside green boxes to the right of the circles for the corresponding day back in time). The circles are filled with a grey shading that represents the mean plume altitude [m]. The blue crosses near Iceland mark the aircraft measurement location.